*Supporting Information*

# Ligand Binding-Induced Structural Changes in the $M_2$ Muscarinic Acetylcholine Receptor Revealed by Vibrational Spectroscopy

Kota Katayama[†,‡,a], Kohei Suzuki[†,a], Ryoji Suno[§,a], Hirokazu Tsujimoto[‖], So Iwata[‖], Takuya Kobayashi[§,⊥], Hideki Kandori[†,‡,*]

[†] Department of Life Science and Applied Chemistry, Nagoya Institute of Technology, Showa-ku, Nagoya 466-8555, Japan

[‡] OptoBioTechnology Research Center, Nagoya Institute of Technology, Showa-ku, Nagoya 466-8555, Japan

[§] Department of Medical Chemistry, Kansai Medical University, Hirakata 573-1010, Japan

[‖]Department of Cell Biology and Medical Chemistry, Graduate School of Medicine, Kyoto University, Kyoto 606-8501, Japan

[⊥] Japan Agency for Medical Research and Development, Core Research for Evolutional Science and Technology (AMED-CREST), Tokyo 100-0004, Japan

Email: kandori@nitech.ac.jp

**Methods:**

**Protein expression, purification and reconstitution.** The $M_2R$ fused with BRIL at ICL3 position ($M_2R$) was expressed and purified as described previously,[1] except for some minor modifications for reconstitution into the membrane. Briefly, C-terminally His-tagged M2-BRIL with the hemagglutinin (HA) signal sequence followed by an N-terminal FLAG tag was expressed in Sf9 insect cells. Cells were infected at a density of 3–4 × $10^6$ cells/mL and grown for 48 h at 27°C. Sf9 cells were lysed by osmotic shock in the presence of 10 μM atropine (Sigma-Aldrich). The lysed membranes were solubilized with a buffer of 30 mM HEPES-NaOH (pH 7.5), 0.75 M NaCl, 5 mM imidazole, 1% (w/v) n-dodecyl-β-D-maltopyranoside (DDM; anatrace), 0.2% sodium cholate (Wako), 1 mg $ml^{-1}$ iodoacetamide (Dojindo), and Complete Protease inhibitor (Roche) for 1 hour at 4°C. The supernatant was isolated by ultracentrifugation for 30 min at 140,000 × g and incubated with Ni-NTA Sepharose Superflow resin (Qiagen) overnight at 4 °C. After binding, the resin was washed with Ni-NTA wash buffer: 30 mM HEPES-NaOH (pH 7.5), 0.75 M NaCl, 0.1% (w/v) DDM, 0.02% (w/v) sodium cholate, 5 mM imidazole and 10 μM atropin. The protein was then eluted with Ni-NTA elution buffer: 30 mM HEPES-NaOH (pH 7.5), 0.75

M NaCl, 0.1% (w/v) DDM, 0.02% (w/v) sodium cholate, 5 mM imidazole and 10 μM atropine, 500 mM imidazole. The eluate was supplemented with 2 mM calcium chloride and loaded onto an anti-FLAG M1 affinity resin (Sigma). The receptor was eluted from the anti-FLAG M1 affinity resin with a buffer of 20 mM HEPES-NaOH (pH 7.5), 0.1 M NaCl, 0.01% (w/v) DDM, 10 μM atropine, 0.2 mg $ml^{-1}$ FLAG peptide and 5 mM EDTA. Finally, protein was purified by Superdex 200 Increase size exclusion column (GE Healthcare) in a buffer of 20 mM HEPES-NaOH (pH 7.5), 0.1 M NaCl, 0.01% (w/v) DDM.

For ATR-FTIR measurements, detergent-solubilized $M_2R$ was reconstituted into asolectin liposomes with a 20-fold molar excess. The detergent molecule was removed by incubation with Bio-beads SM-2 (Bio-Rad, CA, USA). After removal of Biobeads, the lipid-reconstituted $M_2R$ was collected by ultracentrifugation. After several cycles of wash/spin, lipid-reconstituted $M_2R$ was suspended in a buffer composed of 5 mM phosphate (pH 7.5), 10 mM KCl.

**Measurement of ligand binding-induced difference ATR-FTIR spectroscopy.** A 2 μL aliquot of the lipid-reconstituted $M_2R$ suspensions was placed on the surface of a silicon ATR crystal (three internal total reflection). After it was dried in a gently natural drying, the sample was rehydrated with a solvent containing 200 mM phosphate (pH 7.5) buffer with 140 mM NaCl, 3 mM $MgCl_2$ at a flow rate of 0.6 mL $min^{-1}$ through a flow cell, of which the temperature was maintained at 20 °C by circulating water. ATR-FTIR spectra were first recorded at 2 $cm^{-1}$ resolution, using an FTIR spectrometer (Bio-rad FTS7000, Agilent, CA, USA) equipped with a liquid nitrogen-cooled MCT detector (an average of 768 interferograms). After the FTIR spectrum had been recorded in the second buffer with 1 mM ligand, the difference FTIR spectrum was calculated by subtracting the data obtained for the first and second buffer. The cycling procedure was repeated two to seven times, and the difference spectra were calculated as the average of the presence minus absence spectra of ligand. The spectral contributions of the unbound ligand, the protein/lipid shrinkage, and water/buffer components were corrected (see Main text in detail). In order to avoid non-specific signal, we consider the signal before circulating the buffer (with ligand) and after circulating the buffer (without ligand), and we confirm that the signal returns to baseline (Figure S8). For the measurements in $D_2O$ media, the perfusion buffers with the same composition were prepared using deuterium oxide (99 atom % D, Sigma-Aldrich) instead of deionized water, which was adjusted at pD 7.5, assuming the pD value equals $pH_{meter\ reading} + 0.4$.[2] The dissociation constant ($K_d$) for acetylcholine binding was estimated from the concentration dependence of acetylcholine on the IR band intensities of amide-I band at 1666-1656 $cm^{-1}$, amide-II band at 1555-1545 $cm^{-1}$, and ester C=O stretch at 1741 $cm^{-1}$. These band intensities were fitted by Hill equation, where Hill coefficient value was fixed to 1.0.

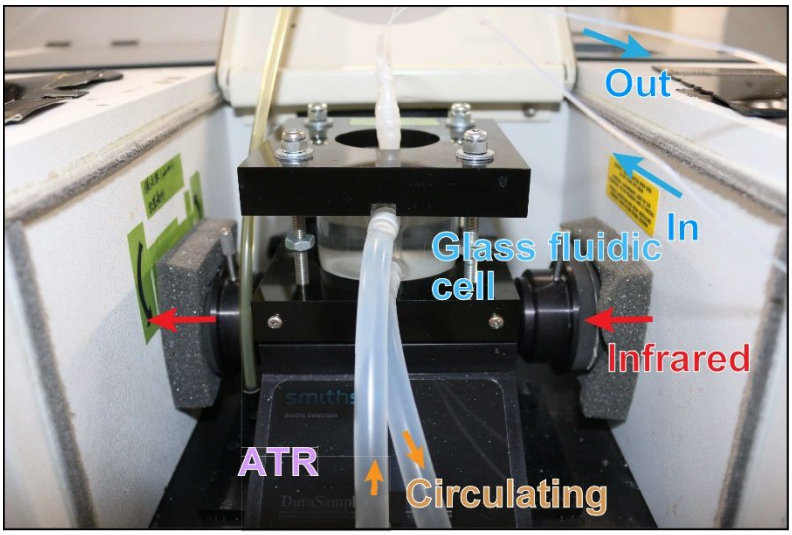


**Figure S1 Picture of the buffer-exchange system through glass fluidic cell.** The ATR chamber was mounted on the stainless plate with a silicon crystal in the DuraSamplIR II ATR accessory. The connecting tube allows to regulate the temperature around sample deposit place by circulating water.

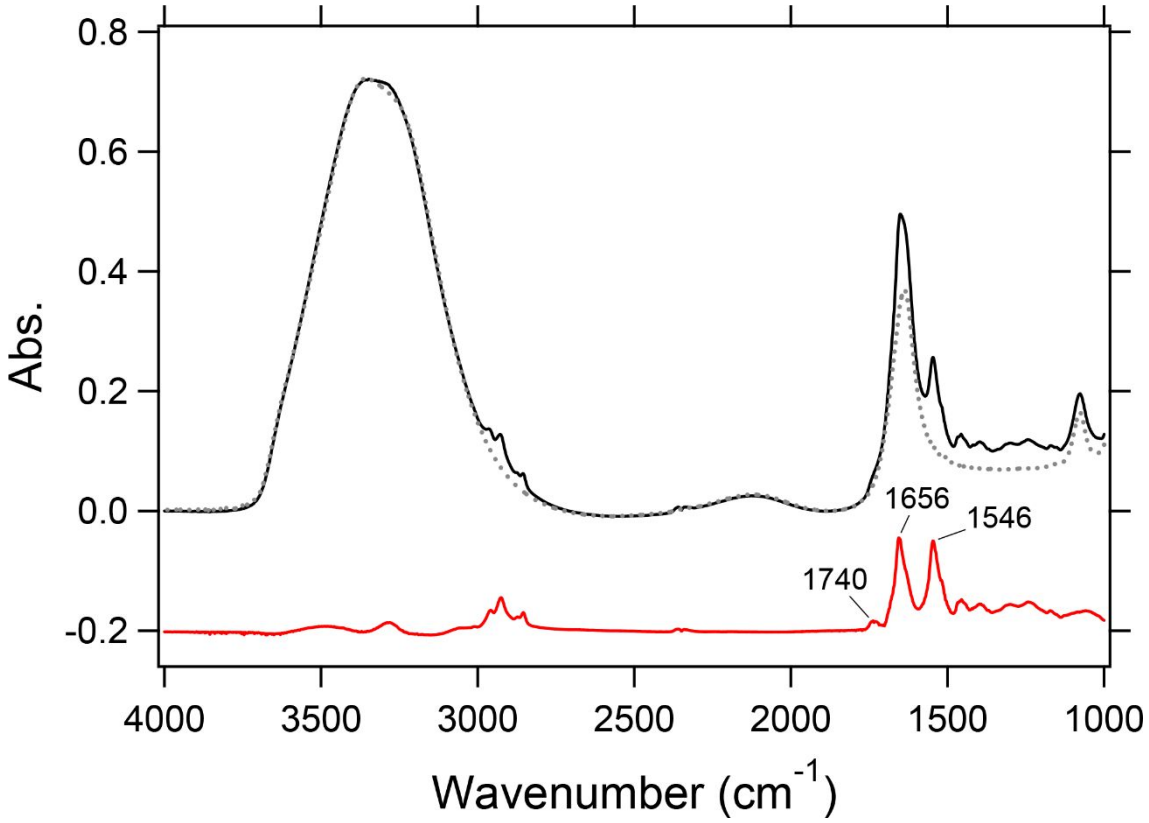


**Figure S2 Absolute infrared absorption spectra of the $M_2R$ sample adsorbed on the ATR crystal and suspended in buffer containing 200 mM phosphate (pH 7.5), 140 mM NaCl, and 3 mM $MgCl_2$.** The spectrum without the $M_2R$ sample is drawn with the dotted line. The absolute spectrum of $M_2R$ sample without the buffer contribution was shown in the bottom panel. A typical protein backbone IR absorption of amide-I and amide-II band were observed at 1656 and 1546 $cm^{-1}$, respectively, and the lipid reconstitution of $M_2R$ was confirmed by a band at 1740 $cm^{-1}$ originated from the carbonyl C=O stretch of lipid.

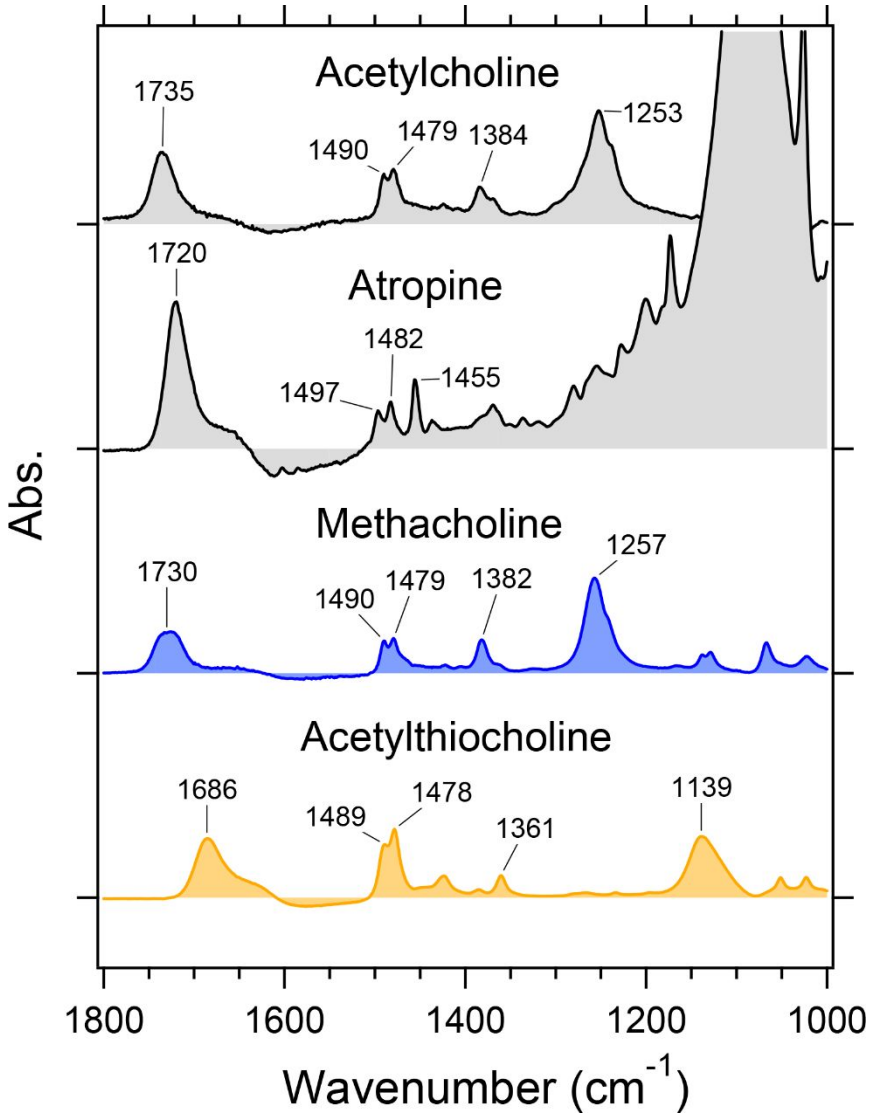


**Figure S3 Comparison of IR absorption of each ligand.** Ligand binding-induced difference ATR-FTIR spectroscopy without protein in the 1800-1000 $cm^{-1}$ region. The intense peaks at 1735 $cm^{-1}$ (acetylcholine), 1720 $cm^{-1}$ (atropine), 1730 $cm^{-1}$ (methacholine), and 1686 $cm^{-1}$ (acetylthiocholine) are originated from ester C=O stretches, respectively. One division of the y-axis corresponds to 0.00035 absorbance unit.

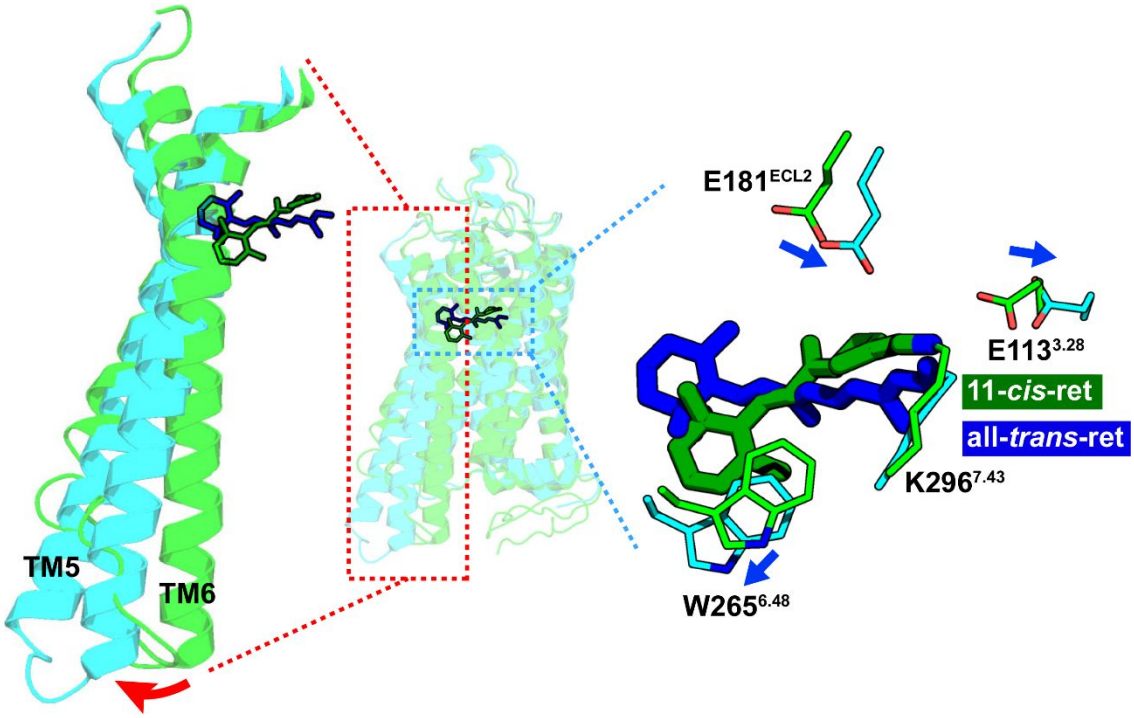


**Figure S4 Comparison of crystal structures of inactive, 11-*cis*-retinal bound dark state (green, PDB: 1U19[3]), and active, all-*trans*-retinal bound Meta-II state (blue, PDB: 3PQR[4]) of bovine rhodopsin.** Conformational changes of both TM6 and retinal binding pocket are shown.

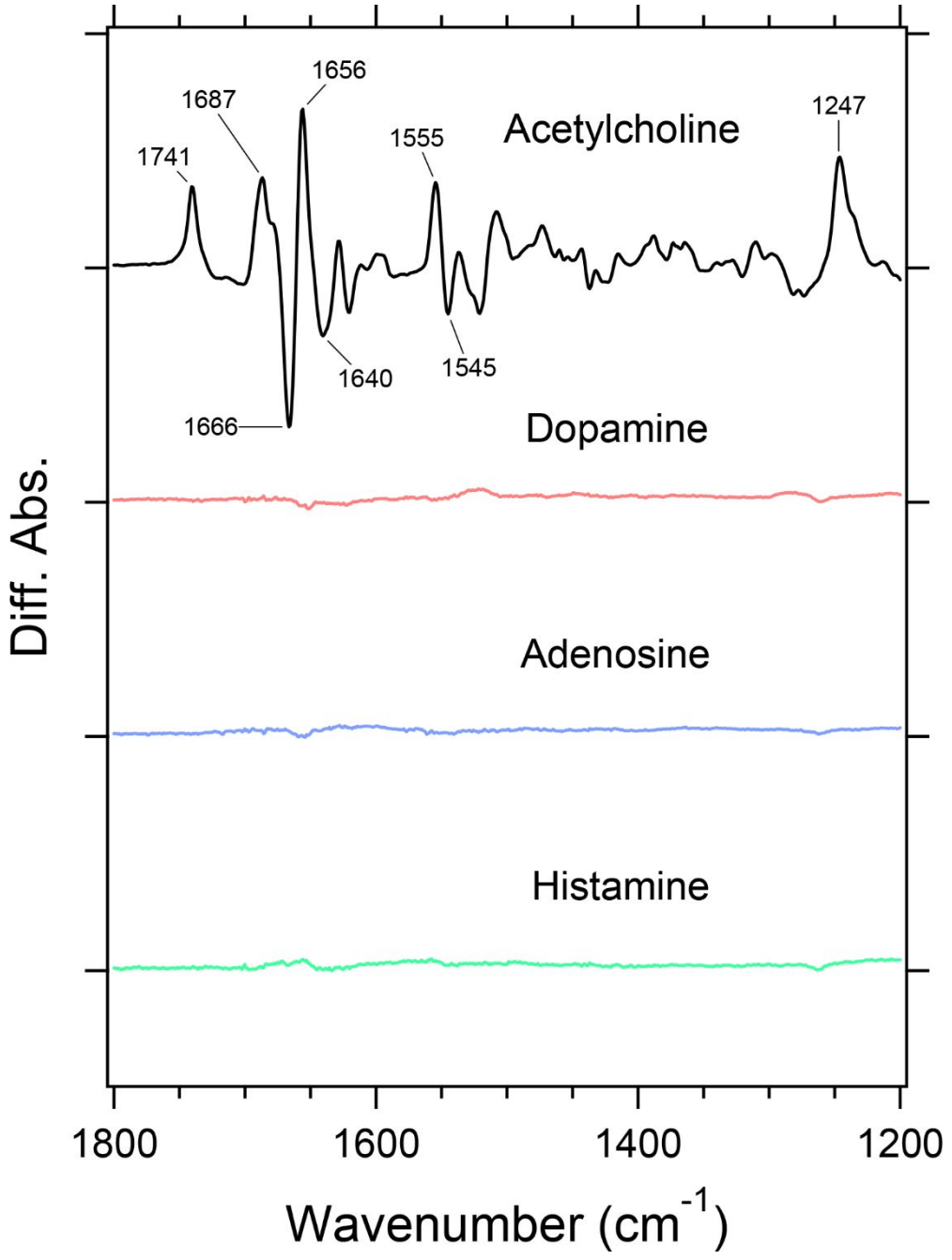


**Figure S5 Effect of $M_2R$ non-specific ligand containing tertiary amine group.** Difference ATR-FTIR spectra upon $M_2R$ non-specific ligand binding such as adenosine, dopamine, and histamine, all of which have tertiary amine group. One division of the y-axis corresponds to 0.0015 absorbance unit.

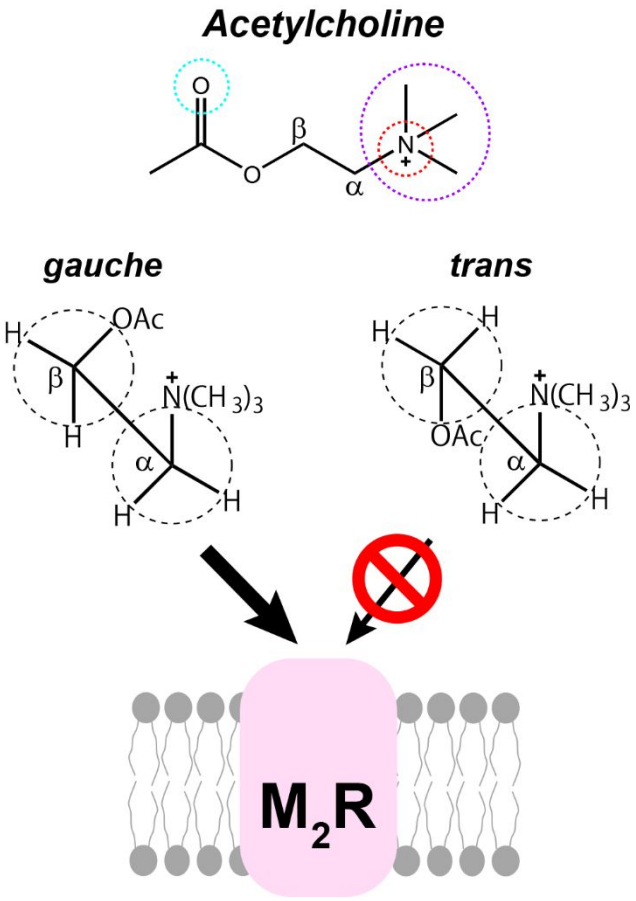


**Figure S6 Stereochemistry of acetylcholine in $M_2R$.**

A diagrammatic illustration of the stereochemistry of acetylcholine by $M_2R$ recognition.

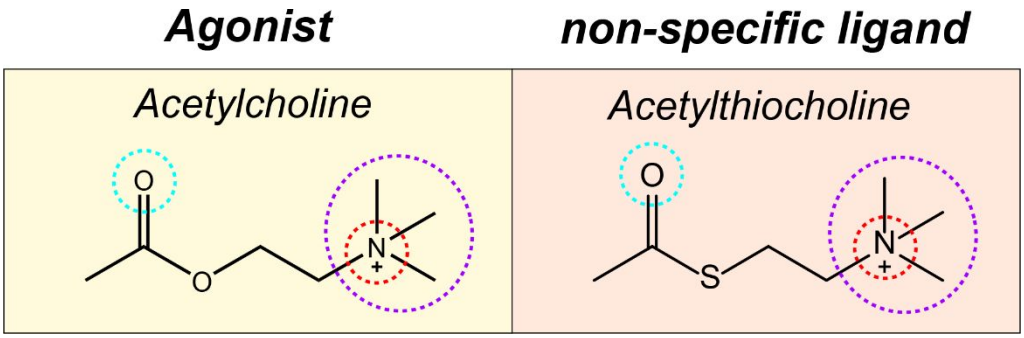


**Figure S7 Chemical structures of acetylcholine and acetylthiocholine.** Common features among each ligand are marked by dashed circles.

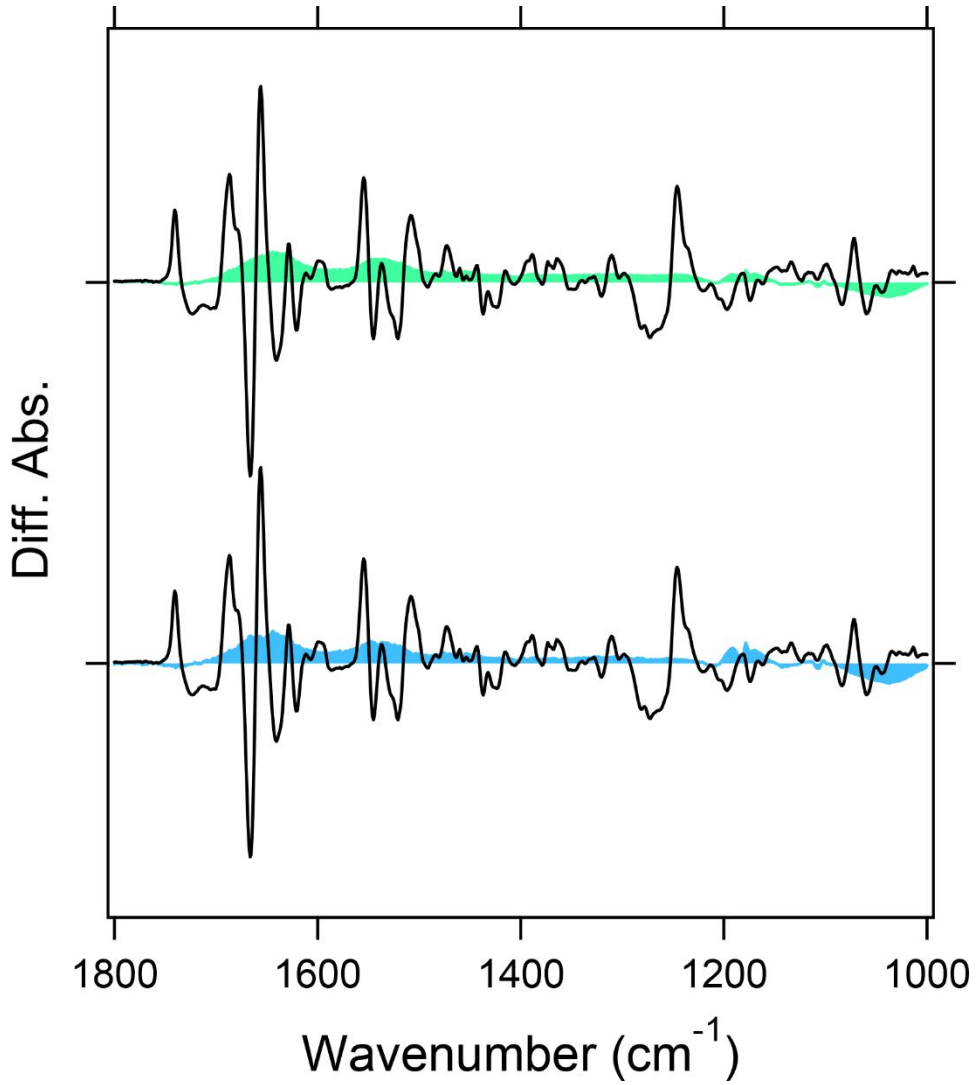


**Figure S8 Effect of non-specific IR signal on the ligand binding-induced difference ATR-FTIR spectroscopy.** The influence of non-specific IR signal and protein/buffer fluctuation was evaluated by calculating before circulating the buffer (with ligand) and after circulating the buffer (without ligand). The signal intensity originated from fluctuation (green and blue filled lines) were almost baseline.

**Reference**


(1) Suno, R.; Lee, S.; Maeda, S.; Yasuda, S.; Yamashita, K.; Hirata, K.; Horita, S.; Tawaramoto, M.; Tsujimoto, H.; Murata, T.; Kinoshita, M.; Yamamoto, M.; Kobilka, B. K.; Vaidehi, N.; Iwata, S.; Kobayashi, T. Structural insights into the subtype-selective antagonist binding to the $M_2$ muscarinic receptor. *Nat. Chem. Biol.* **2018**, *14*, 1150-1158.

(2) Glasoe, P. K.; Long, F. A. Use of glass electrodes to measure acidities in deuterium oxide. *J. Phys. Chem*. **1960**, *64*, 188-190.

(3) Okada, T.; Sugihara, M.; Bonder, A-N.; Elstner, M.; Entel, P.; Buss, V. The retinal conformation and its environment in rhodopsin in light of a new 2.2 Å crystal structure. *J. Mol. Biol.* **2004**, *342*, 571-583.

(4) Choe, H-W.; Kim, Y. J.; park, J. H.; Morizumi, T.; Pai, E. F.; Krauss, N.; Hofmann, K. P.; Scheerer, P.; Ernst, O. P. Crystal structure of metarhodopsin II. *Nature* **2011**, *471*, 651-655.